OPTO-ELECTRONICS REVIEW **14**(1), 47–54

Advanced features of SCD's uncooled detectors

A. FRAENKEL*, U. MIZRAHI, L. BYKOV, A. ADIN, E. MALKINSON, Y. ZABAR, D. SETER, Y. GEBIL, and Z. KOPOLOVICH

Semi Conductor Devices (SCD), P.O. Box 2250, Haifa 31021, Israel

SCD has recently presented an uncooled detector product line based on the high-end VO_x bolometer technology. The first FPA launched, BIRD, is a 384×288 (or 320×240) configurable format with 25 µm pitch. Typical NETD values for these FPAs range at 50 mK with an F/1 aperture and 60 Hz frame rate. These detectors also exhibit a relatively fast thermal time constant of approximately 10 ms.

In this paper we elaborate on the special advanced features that were incorporated within the ROIC and supporting algorithms. In this framework we have addressed two important issues: the power consumption and the time span between shutter activations. Minimum power consumption is a critical issue for many un-cooled applications. SCD has addressed this by introducing the "power-save" concept accompanied with flexible dilution architecture. The paper will present recent results exhibiting the various advantages.

One of the limiting factors on the performance of uncooled detectors is their vulnerability to ambient drift. Usually, even minor temperature fluctuations are manifested as high residual non-uniformity (RNU) or fixed pattern noise (FPN). As a result frequent shutter operations must be applied, with the risk of blocking the scenery in critical time frames. The challenge is thus twofold: to increase the time span between shutter corrections and achieve better control of its activation.

For this purpose BIRD provides two complementing mechanisms: A real-time (frame-by-frame) ambient drift compensation accompanied by an RNU prediction mechanism. The paper will discuss these features in detail and present illustrative system implementations.

Keywords: uncooled FPA, VO_x technology, "power-save", ambient drift compensation, RNU prediction.

1. Introduction and background

Uncooled infrared detectors are being developed for a wide range of thermal imaging applications. These detectors have significant cost, size, weight, power and reliability advantages over cryogenic FPAs [1,2].

The development work on uncooled arrays at SCD has been focused on the high-end market segment. Therefore the superior VO_x micro-bolometer technology was chosen. Additionally, during the development phase, a considerable effort was invested in reducing the power consumption and minimizing the spatial non-uniformity or RNU.

High performance detectors demand tight FPA stabilization using a thermo-electric-cooler (TEC). However, under extreme environmental conditions the TEC will consume excessive power. The "power save" architecture described herein, in which the die temperature can be stabilized to the ambient temperature, reduces power consumption with minimal performance degradation. In particular, it still maintains low and stable spatial noise. Combining this feature with smart dilution mechanisms can reduce the total detector power dissipation well below 250 mW.

Many of the applications in the IR are limited by the spatial non-uniformity or RNU [3]. This issue was thoroughly investigated by us both theoretically and experimentally. It was found out that besides the well-known electronics drift and $1/f$ noise, un-cooled detectors are also sensitive to other drift mechanisms, among them is ambient drift.

Usually, even minor temperature fluctuations are manifested as high residual non-uniformity (RNU) or fixed pattern noise (FPN). As a result frequent shutter operations must be applied, with the risk of blocking the scenery in critical time frames. The challenge is thus twofold: to increase the time span between shutter corrections and achieve better control of its activation. For this purpose BIRD provides two complementing mechanisms: A real-time (frame-by-frame) ambient drift compensation accompanied by an RNU prediction mechanism.

The first section of the paper summarizes briefly the basic BIRD's architecture and performance. In the following section we describe the "power-save" concept and measurement results. This is followed by a detailed description of the RNU prediction and compensation mechanisms and the way they are combined in specific scenarios.

*e-mail: ramifr@scd.co.il

The paper presented there appears in *Infrared Photoelectronics*, edited by Antoni Rogalski, Eustace L. Dereniak, Fiodor F. Sizov, Proc. SPIE Vol. 5957, 59570N (2005).

2. BIRD architecture and performance

2.1. Microbolometer technology

The microbolometers are fabricated on a 6″ Silicon ROIC wafer using the surface micromachining technique. Each pixel consists of a SiN_x membrane suspended above the substrate. The membrane is supported by two legs that provide the thermal isolation and electrical contacts. A thin VO_x layer serves as the temperature sensitive material, exhibiting high TCR (–2.4%/K), excellent uniformity and negligible $1/f$ contribution. The overall absorption efficiency is well above 80%.

2.2. Package design

The detector is packaged in a high vacuum metallic case, designed to ensure the vacuum level for at least 15 years (in suitable ambient temperature). The package measuring 41×30×7 mm is shown in Fig. 1. The base of the package is used as mounting surface and features high accuracy design in order to ensure proper parallelism. Thus, both the front and rear face can be used as optical bench for mounting. Special I/O pins are connected to internally mounted Getters that can be re-activated by the user to ensure vacuum integrity for very long periods. The external resistance-temperature-detector (RTD) is mounted near the optical filter in a special cavity and is connected via isolated wires to special I/O pins. It enables on-line measurements of the case temperature. The package was tested to withstand temperature cycles, random and sine vibration, tenths of thousands of shocks showing no degradation of package integrity and/or detector performance.

Fig. 1. Photograph of the BIRD package.

2.3. ROIC architecture

The CMOS readout integrated circuit (ROIC) block diagram is shown in Fig. 2. It is fabricated with SCD's well established 0.5 micron double-poly, triple metal CMOS process [4]. The ROIC consists of an internal timing machine with a single clock that facilitates the electrical interface. The on-chip 10-bit compensation minimizes the coarse non-uniformity to less than 200 mV (p-t-p), which is < 10% of the useful dynamic range. Following is a list of some unique features that enhance the detector's flexibility and operating range:

- software configurable array size,
  - horizontal configuration by de-selection of columns,
  - vertical configuration by row random access,
- accommodation (FFF) of two detector pixels,
  - "slow" pixel for surveillance applications: 12-ms time constant,
  - "fast" pixel for missile applications: 5-ms time constant,
- 16-level programmable on-chip gain selection for wide FPA and ambient temperature span,
- differential architecture with high common mode rejection ratio (CMRR) to noise and bias fluctuations,
- communication feedback for debugging capabilities,
- full camera BIT (built in testing) mode,
- pixel overheating protection,
- single video output,
- blind pixel redundancy for higher yield and lower cost of ownership.

2.4. Basic performance

The main performance characteristics and specification are summarized in Table 1. All the radiometric results are per the following conditions: $F/1$, 30/60 Hz (or 25/50 Hz for the 384×288 format), and 300 K FPA and scene temperatures.

Figure 3 shows a representative temporal *NETD* ($F/1$ and 50 Hz) histogram and accumulative distribution. The median value is 46 mK with more than 80% of the array lower than 50 mK. These results were repeated on hundreds of samples by now, with the average operability exceeding 99%.

In Fig. 4 we show a typical distribution of the array thermal time constant measured with a mechanical shutter. The average value is roughly 8.7 ms, ensuring a large enough margin even for the "slower" pixels in the distribution.

Another important figure of merit is the dynamic range. The "effective" linear range (following compensation) is roughly 3 V. The on-chip gain selection provides additional degree of freedom, enabling up to 200°C target DR for the lowest gain. Figure 5(a) exhibits the intra-scene instantaneous dynamic range which is roughly 100°C for the specific gain level chosen. In this particular case, the detector was compensated against a 25°C target with V_{set} = 2.5 V (which is the centre of the effective DR). It should be stressed, however, that by varying the compensation set point one can achieve a practically "infinite" non-simultaneous range. Since the ROIC is equipped with 16 discrete gain levels, it provides a flexible tradeoff between DR and temporal *NETD* (higher electronic gain will reduce the total noise).

Finally, the "effective" range under varying ambient (constant 25°C target) is shown in Fig. 5(b). The detector can withstand ±5°C variation while keeping an effective target range of 40 degrees.

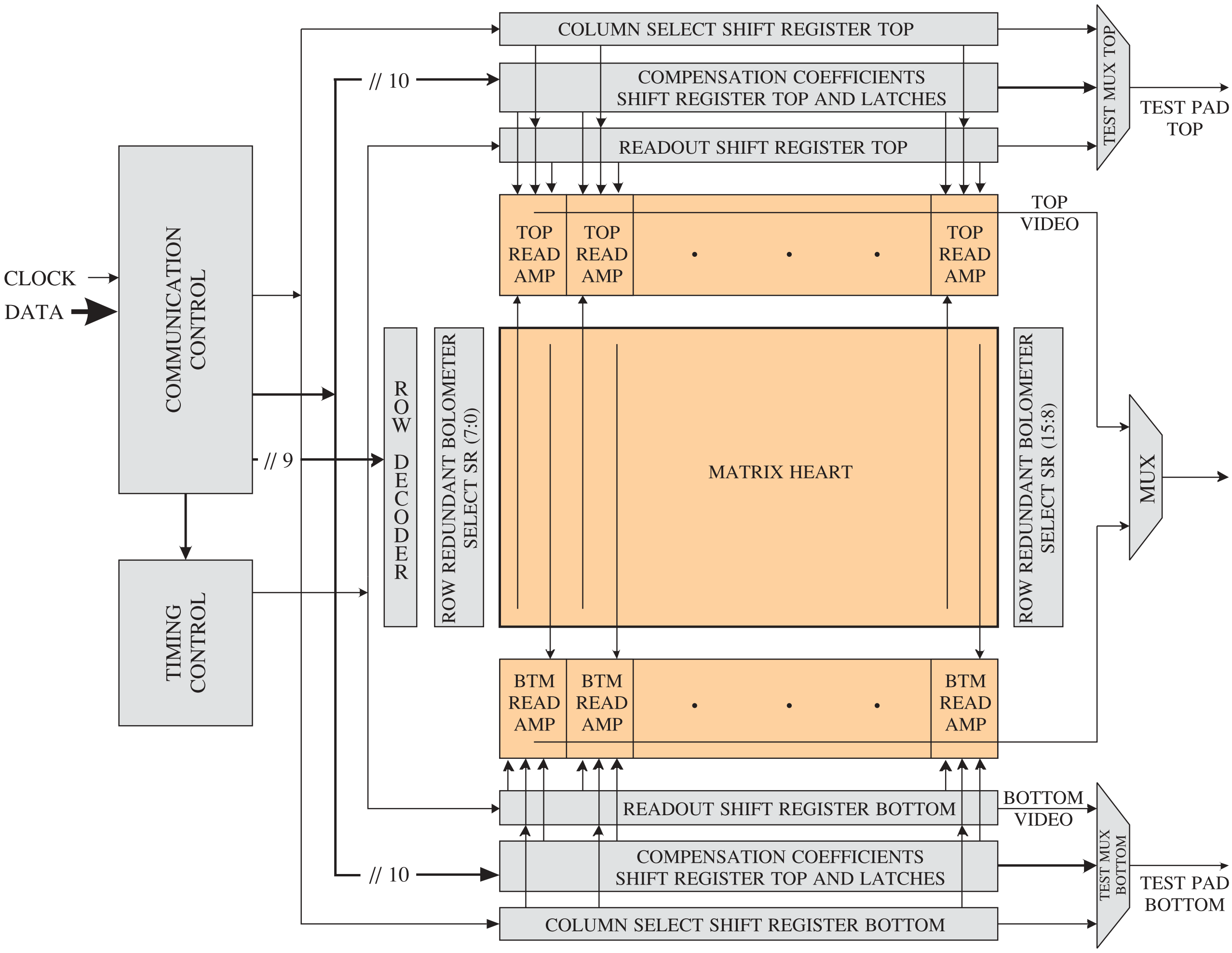

Fig. 2. Block diagram of the ROIC.

Table 1. Performance characteristics of the 25-μm detector.

Parameter	Performance
Array size	384×288 (320×240, 160×120 configurable)
Pitch	25 μm
Spectral band	8–14 μm
Thermal time-constant	5 or 12 ms (typically 10) for "fast" and "slow" pixels
Temporal *NETD* (*F*/1, 30Hz)	< 35 mK @ 12 ms (50 mK at 60 Hz) < 50 mK @ 5 ms (70 mK at 60 Hz)
Intra-scene DR	> 100 K
Coarse non uniformity (after compensation)	< 200 mV (p-t-p)
Power dissipation	< 200 mW (excluding TEC)
Package weight	< 20 gram
Pixel operability	> 99%
Nominal operating temperature	25°C
Ambient range	–40°C – 70°C

3. The "power-save" concept

3.1. Power dissipation

The "power save" concept was introduced a few months ago [1], with preliminary results. We have also detailed its advantages over the "TEC-less" architecture. In this section we elaborate further with special stress on the reduced power consumption and the "mission readiness".

While optimized for 25°C FPA temperature, the detector was designed to withstand a large tolerance in bolometer resistance, dynamic heating, and TCR. The temporal *NETD* is below 60 mK for the entire region (–35°C to

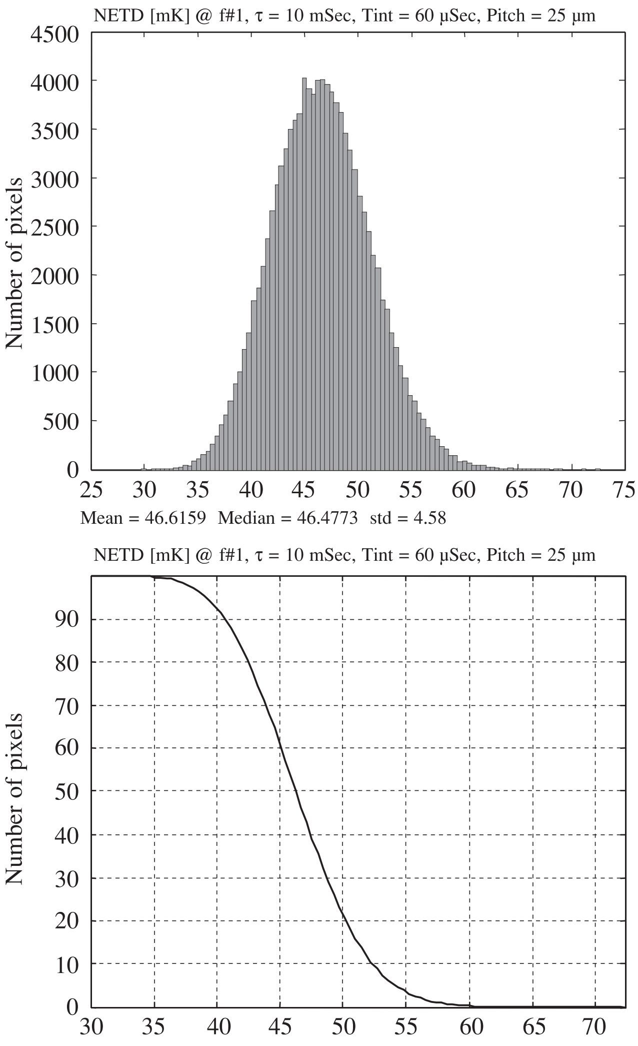

Fig. 3. Temporal *NETD* histogram and accumulative distribution.

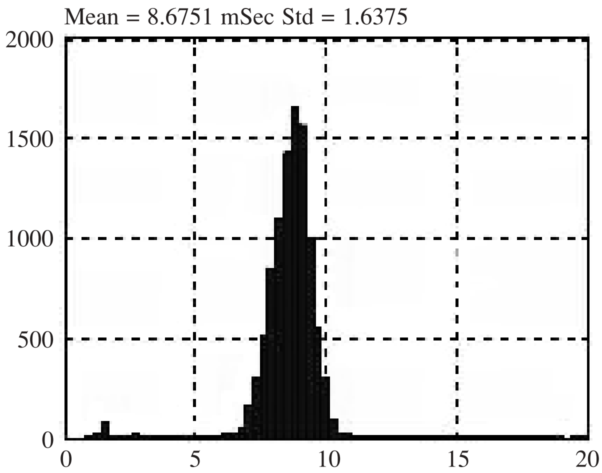

Fig. 4. Typical distribution of the thermal time constant.

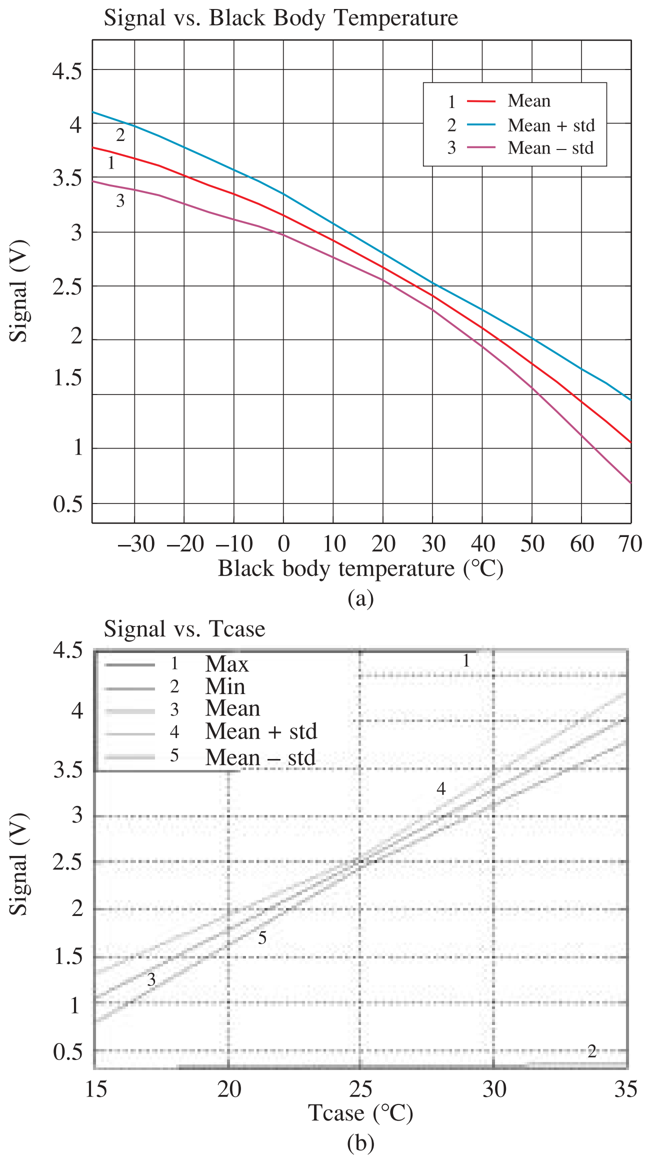

Fig. 5. Simultaneous intra-scene DR (constant ambient) (a), effective intra-scene DR (constant target) (b).

+65°C) as depicted in Fig. 6. Special provisions and on-chip gain selection reduce the coarse non-uniformity after compensation below 300 mV (p-t-p) throughout, while still maintaining 100 K intra-scene dynamic range.

The detector's cumulative power dissipation is contributed by several sources: the FPA (ROIC + pixels), the TEC and excess system electronics (which is out of the scope of this paper). The full array (EUR format) contributes roughly 200 mW. A 50% column dilution (e.g., only odd or even columns) will reduce it to 130 mW. By applying also row dilution, an additional reduction of 25 mW is achieved. The detector transits “smoothly” between full and diluted images with only offset (shutter) correction. Hence, in a typical surveillance application, the system can reduce power by operating in the dilution mode and upon initial detection merge to the full format.

Figure 7 presents the excess TEC dissipation under the “power save” scenario, where the FPA is stabilized to the ambient temperature. As expected, the excess dissipation rises in the low temperature regime but is still below 150 mW even under the most extreme conditions. Combining

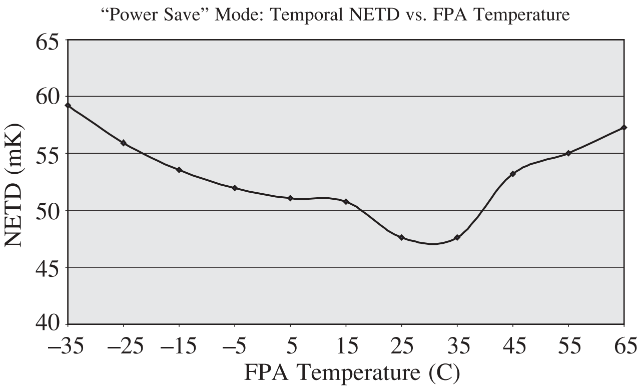

Fig. 6. Temporal *NETD* vs. FPA temperature within the "power-save" mode.

this information with the dilution data we can conclude the following:
- detector power dissipation at full format with "power save" is lower than 350 mW,
- with partial (column) dilution and "power save" < 280 mW,
- with full dilution and "power save" < 250 mW.

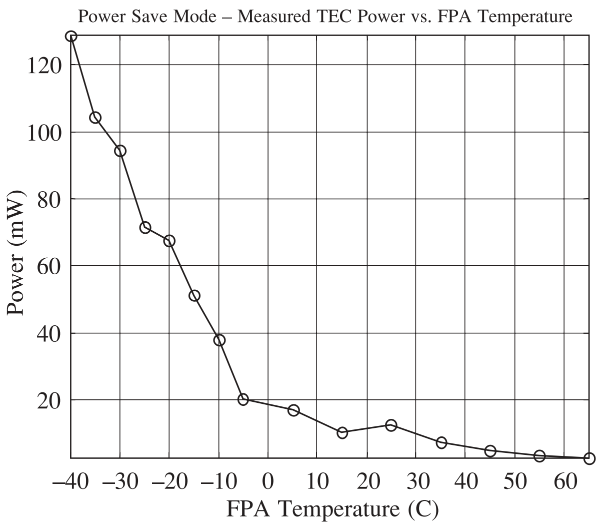

Fig. 7. Excess TEC power dissipation for the "power-save" mode ($T_{FPA} = T_{ambient}$).

3.2. Mission readiness

In the previous section we elaborated on the power reduction advantages of the "power-save" mode. Here, we describe another merit which is the so-called "mission readiness". When an uncooled detector is designed to operate at a constant FPA temperature (e.g., 25°C), then under extreme ambient conditions it might need several minutes to stabilize. During this period the detector is virtually inactive.

In contrast, when using the "power-save" mode this period is much shorter since the FPA stabilizes to the instantaneous ambient temperature or its vicinity. Furthermore, even during this short transition period the detector will supply a reasonable image.

In order to verify this point, we have performed a smooth "power-save" transition varying the FPA temperature between 25 and 40°C. The FPA was corrected (compensation and NUC) at 25°C and then heated gradually to 40°C with a ~2.5°C/minute ramp. The 25°C compensation and gain correction arrays were used throughout. The shutter was activated once every minute.

Figure 8 shows representative images captured (8 frames per image) during this interval. The instantaneous FPA temperature is added for reference on each image.

Our conclusions are as follows:
- with proper TEC controller and several shutter activations (10 frames per activation) the detector can be tuned smoothly up to ±15°C while still maintaining reasonable image quality,
- the compensation array may be valid for a ±15°C FPA temperature variation (although we recommend a new table every ~10 degrees in order to maintain the full target dynamic range),
- the gain correction array varies slowly and smoothly with the FPA temperature.

Finally, it should be noted again that all the above provisions make our detector also fit for "TEC-less" operation mode. However, the "power-save" concept (especially when used with discrete points) reduces the spatial noise, computational complexity and the demands for on-chip voltage regulation [5].

4. RNU prediction and compensation

Unlike cryogenic detectors that are virtually isolated from the ambient with a cold shield, uncooled arrays are extremely sensitive to ambient variations. The detector package is mounted and interfaced to a heat-sink within the camera, which in turn closely follows the ambient temperature. For $F/1$ system applications the interior parts of the camera can contribute as much as four times the scene (target) flux.

During routine system operation the ambient temperature drifts. It can be either a slow and gradual drift (e.g., surveillance systems) or much sharper (e.g., fire fighting or missile seekers). In practice, each pixel of the array has a different FOV (field of view) of the camera body, thus experiencing different flux. This is added to the inherent process induced non-uniformity. As the temperature drifts, each pixel drifts slightly differently, destroying the low RNU (residual non uniformity) achieved during two point correction.

The compensation of this effect is one of the most challenging problems facing uncooled system designers. It is especially difficult during the initial stabilization period. The common practice is to perform frequent offset corrections with an optical shutter [6].

However, this method suffers from few major drawbacks: the shutter might block the scenery in a critical time frame for various applications. Secondly, the image deteriorates between subsequent shutter operations, forming a "saw

Fig. 8. Representative images captured during "power-save" transition.

tooth" RNU pattern. In addition, the shutter being the only moving part of the camera limits the system reliability.

In order to circumvent these difficulties and facilitate system-level solutions, SCD has introduced a real-time frame-by-frame non-uniformity prediction and correction mechanisms. The scheme utilizes special auxiliary data that is streamed as an integral part of the video line. It is than incorporated (on a frame-to-frame basis) in the standard NUC block, without any additional temporal or spatial manipulations.

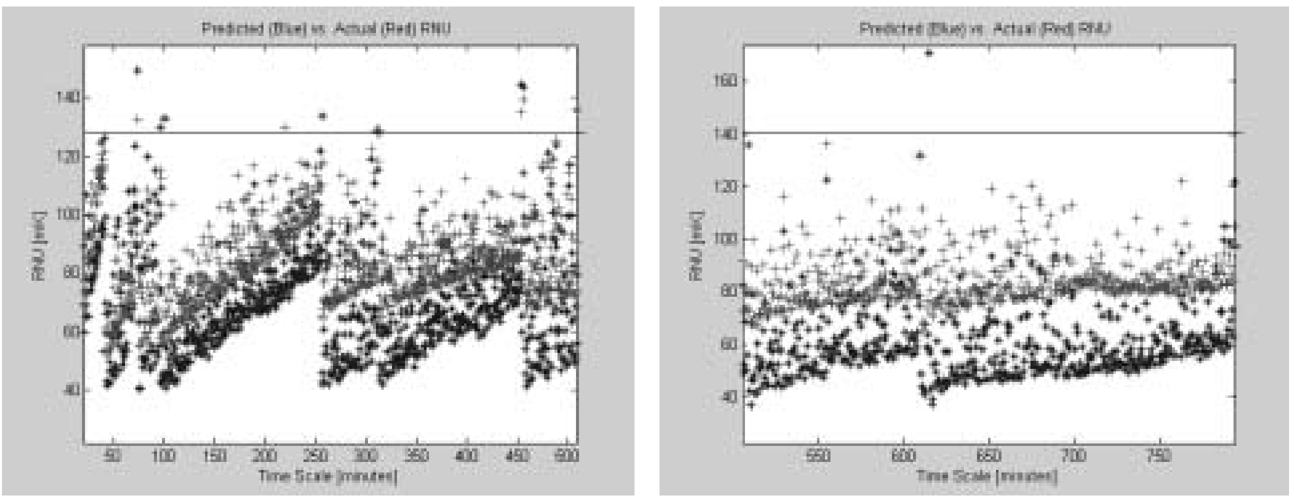

Fig. 9. RNU prediction vs. array RNU (shutter limit at 125 mK) – variable ambient (a) and stable ambient (b).

Fig. 10. BIRD imagery (50-mm lens) illustrating the real-time ambient compensation (right image) after 5.25°C drift during 90 min with no shutter activation.

Figures 9(a) and 9(b) exhibit the RNU prediction mechanism. The system calculates the standard deviation of the special RNU prediction columns and activates the shutter when a pre-determined threshold is reached. Evidently, there is a tight correlation between the predicted and actual array RNU. Due to the existence of ambient drift compensation mechanism, even with variable ambient the shutter is activated only few times during an eight hour duration. When the module is put in a stabilized environmental chamber, the shutter is not activated for more than 5 hours (!). This demonstrates once again the high temporal stability of SCD's VO_x technology.

Next, we move to the ambient compensation mechanism. Figure 10 shows images captured roughly 90 minutes after a two point correction with no shutter activation. During that period the ambient drifted spontaneously ~5 degrees. In the upper left-hand image, only the original correction is applied. There is a perceptible non-uniformity pattern especially in the periphery. This is due to the fact that the edges are affected the most by the ambient variation. In the upper right-hand image the real-time auxiliary mechanism was applied and the image is considerably smoother. The auxiliary mode provides an order of magnitude improvement in the non-uniformity when viewing a uniform black-body.

In order to obtain a more quantitative perspective, we have repeated the entire experiment against a uniform black-body source. The measurement proceeded for almost 5 hours with 4 degrees drift. The results, shown in Fig. 11, exhibit again order of magnitude reduction in RNU (from 1 K to 100 mK) when utilizing the compensation mechanism. It should be noted that the RNU curve closely follows the ambient drift, indicating that this is indeed the dominant contributor to the spatial noise (rather than e.g. the 1/*f* pixel noise).

In conclusion, the combined RNU prediction and compensation mechanism is a very powerful tool, especially so for unattended sensor applications [7], where the idle time (due to e.g. shutter activations) should be drastically minimized.

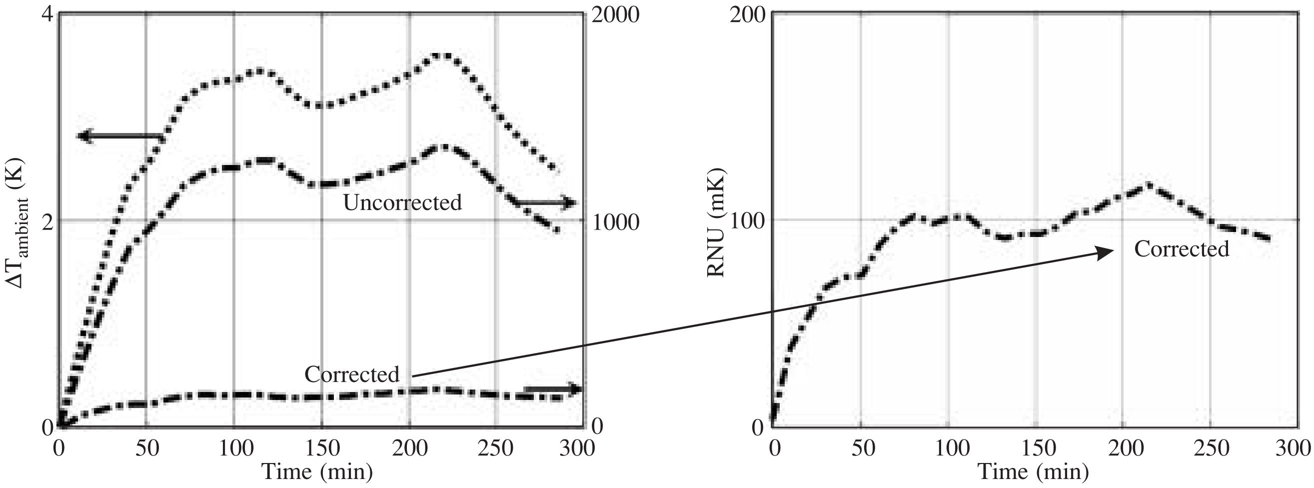

Fig. 11. RNU vs. $\Delta T_{ambient}$ with two point correction (left-hand graph) and the additional auxiliary correction mechanism (right-hand graph). Time span is roughly 300 min.

5. Conclusions

In this paper, we elaborated on the special advanced features that were incorporated within the ROIC and supporting algorithms of BIRD. In this framework, we have addressed two important issues: the power consumption and the time span between shutter activations. Minimum power consumption is a critical issue for many uncooled applications. SCD has addressed this by introducing the "power-save" concept accompanied with flexible dilution architecture. The paper presented recent results exhibiting the various advantages.

One of the limiting factors on the performance of uncooled detectors is their vulnerability to ambient drift. As a result frequent shutter operations must be applied, with the risk of blocking the scenery in critical time frames. For this purpose BIRD provides two complementing mechanisms: A real-time (frame-by-frame) ambient drift compensation accompanied by an RNU prediction mechanism. The paper discussed these features in detail and presented illustrative system implementations.

We believe that the various features combined with the basic "high-end" pixel performance make our device suitable for a broad range of military and commercial applications with superior performance and reduced power consumption.

Acknowledgments

The development of the detector was supported by MAGNET, Israeli Trade & Industry Ministry and MAFAT, Israeli Ministry of Defence. We are in debt to the numerous engineers and technicians participating in the project, for their dedicated contribution to the development and characterization of the detector.

References

1. U. Mizrahi, "Uncooled development program at SCD", *Proc. SPIE* **5783**, 551–558 (2003).
2. P.W. Kruse, *Uncooled Thermal Imaging Arrays, Systems and Applications*, SPIE Press, Bellingham, WA (2001).
3. O. Nesher, S. Elkind, A. Adin, I. Nevo, A.B. Yaakov, S. Raichshtain, A.B. Marhasev, A. Magner, M. Katz, T. Markovitz , D. Chen, M. Kenan A. Ganany, J.O. Schlesinger, and Z. Calahorra, "A digital cooled InSb detector for IR detection", *Proc. SPIE* **5074**, 120 (2003).
4. O. Nesher, P.C. Klipstein, and E. Weiss, "Advanced IR detector design at SCD: from D^3C^{TM} to ABCS", *Proc. SPIE* **5359**, 101–110 (2004).
5. P.E. Howard, J.E. Clarke, A.C. Ionescu, C. Li, and A. Frankenberger, "Advances in uncooled 1-mil pixel size focal plane products at DRS", *Proc. SPIE* **5406**, 512–520 (2004).
6. "Performance specification of uncooled B-Kit module", *Night Vision/RSTA*, January 2003.
7. K. Grealish, T. Kacir, B. Backer, and P. Norton, "An advanced infrared imaging module for military and commercial applications", *Proc. SPIE* **5796**, 186–192 (2005).

